BIOCHEMISTRY. For the article "Expression of Globo H and SSEA3 in breast cancer stem cells and the involvement of fucosyl transferases 1 and 2 in Globo H synthesis," by Wen-Wei Chang, Chien Hsin Lee, Peishan Lee, Juway Lin, Chun-Wei Hsu, Jung-Tung Hung, Jin-Jin Lin, Jyh-Cherng Yu, Li-en Shao, John Yu, Chi-Huey Wong, and Alice L. Yu, which appeared in issue 33, August 19, 2008, of *Proc Natl Acad Sci USA* (105:11667–11672; first published August 6, 2008; 10.1073/pnas.0804979105), the authors note that in the Abstract, line 8, "29/31" should have appeared as "29/40." Additionally, in Table 1, last column, second row from the bottom, "77.5" should have appeared as "72.5." These errors do not affect the conclusions of the article. The corrected table appears below.

Table 1. A comparison of Globo H and SSEA3 expression in BCSCs and non-BCSCs

Glycan and population	No. of patients	Positive		
		No.	Range*	% of total
Globo H†				
Total	41	25	14.3–75.2	61.0
Non-BCSCs	41	25	24.4–79.2	61.0
BCSCs	40‡	8	9.7–71.0	20.0
SSEA3†				
Total	40	31	5.9–66.4	77.5
Non-BCSCs	40	29	24.3–70.4	72.5
BCSCs	40	25	5.0–58.4	62.5

Globo H or SSEA3 expression was determined by flow cytometry as described in *Materials and Methods*. BCSCs were defined as $CD45^-CD24^-CD44^+$ cells, and non-BCSCs were defined as the remaining populations of $CD45^-$ cells.

*Range was calculated as percentage of positive cells in total cells.

†Among the 53 tumor samples, 28 were examined for the expression of both Globo H and SSEA3, 13 were tested for Globo H only, and the remaining 12 were tested for SSEA3 only.

‡Tumor cells from 1 of the 41 patients showed an absence of $CD24^-CD44^+$ subpopulation.

www.pnas.org/cgi/doi/10.1073/pnas.0808811105

ECOLOGY. For the article "Magnetic alignment in grazing and resting cattle and deer," by Sabine Begall, Jaroslav Červený, Julia Neef, Oldřich Vojtěch, and Hynek Burda, which appeared in issue 36, September 9, 2008, of *Proc Natl Acad Sci USA* (105:13451–13455; first published August 25, 2008; 10.1073/pnas.0803650105), the authors note that due to a printer's error, on page 13454, right column, in *Analysis of Body Position of Deer (Field Observation)*, the first sentence, "Body position of 2,974 deer (in **227** localities) was recorded in the Czech Republic" should instead read: "Body position of 2,974 deer (in **241** localities) was recorded in the Czech Republic." Additionally, on page 13455, right column, in *Sun Position and Roe Deer Orientation*, the first sentence "The position of the sun could be **deviated** by the exact time of the day" should instead read: "The position of the sun could be **determined** by the exact time of the day."

www.pnas.org/cgi/doi/10.1073/pnas.0809028105

MEDICAL SCIENCES. For the article "Uncovering G protein-coupled receptor kinase-5 as a histone deacetylase kinase in the nucleus of cardiomyocytes," by Jeffrey S. Martini, Philip Raake, Leif E. Vinge, Brent DeGeorge, Jr., J. Kurt Chuprun, David M. Harris, Erhe Gao, Andrea D. Eckhart, Julie A. Pitcher, and Walter J. Koch, which appeared in issue 34, August 26, 2008, of *Proc Natl Acad Sci USA* (105:12457–12462; first published August 18, 2008; 10.1073/pnas.0803153105), the authors note that the author name Brent DeGeorge, Jr., should have appeared as Brent R. DeGeorge, Jr. The author line has been corrected online. The corrected author line and related author contributions footnote appear below.

Jeffrey S. Martini, Philip Raake, Leif E. Vinge, Brent R. DeGeorge, Jr., J. Kurt Chuprun, David M. Harris, Erhe Gao, Andrea D. Eckhart, Julie A. Pitcher, and Walter J. Koch

Author contributions: J.S.M., D.M.H., A.D.E., J.A.P., and W.J.K. designed research; J.S.M., P.R., L.E.V., B.R.D., and E.G. performed research; J.S.M. and D.M.H. contributed new reagents/analytic tools; J.S.M., B.R.D., J.K.C., D.M.H., A.D.E., and W.J.K. analyzed data; and J.S.M. and W.J.K. wrote the paper.

www.pnas.org/cgi/doi/10.1073/pnas.0808974105

MICROBIOLOGY. For the article "Purported nanobacteria in human blood as calcium carbonate nanoparticles," by Jan Martel and John Ding-E Young, which appeared in issue 14, April 8, 2008, of *Proc Natl Acad Sci USA* (105:5549–5554; first published April 2, 2008; 10.1073/pnas.0711744105), the authors note that on page 5550, right column, line 3, "**P:Ca** ratio" should have appeared as "**Ca:P** ratio." This error does not affect the conclusions of the article.

www.pnas.org/cgi/doi/10.1073/pnas.0809132105

PLANT BIOLOGY. For the article "Enhanced photoprotection pathways in symbiotic dinoflagellates of shallow-water corals and other cnidarians," by Jennifer McCabe Reynolds, Brigitte U. Bruns, William K. Fitt, and Gregory W. Schmidt, which appeared in issue 36, September 9, 2008, of *Proc Natl Acad Sci USA* (105:13674–13678; first published August 29, 2008; 10.1073/pnas.0805187105), the authors note that due to a printer's error, on page 13674, right column, second full paragraph, line 6, "maximum quantum yield as $F_v/F_m = F_m - F_0$" should have appeared as "maximum quantum yield as F_v/F_m, where variable fluorescence, $F_v = F_m - F_0$."

www.pnas.org/cgi/doi/10.1073/pnas.0809220105

Purported nanobacteria in human blood as calcium carbonate nanoparticles

Jan Martel*† and John Ding-E Young‡

*Department of Biochemistry and Cellular Molecular Biology, Chang Gung University, 259 Wen-Hua First Road, Kwei-Shan, Tao-Yuan 333, Taiwan, Republic of China; and ‡Department of Cellular Physiology and Immunology, The Rockefeller University, New York, NY 10021

Edited by Norman R. Pace, University of Colorado, Boulder, CO, and approved February 29, 2008 (received for review December 13, 2007)

Recent evidence suggests a role for nanobacteria in a growing number of human diseases, including renal stone formation, cardiovascular diseases, and cancer. This large body of research studies promotes the view that nanobacteria are not only alive but that they are associated with disease pathogenesis. However, it is still unclear whether they represent novel life forms, overlooked nanometer-size bacteria, or some other primitive self-replicating microorganisms. Here, we report that $CaCO_3$ precipitates prepared *in vitro* are remarkably similar to purported nanobacteria in terms of their uniformly sized, membrane-delineated vesicular shapes, with cellular division-like formations and aggregations in the form of colonies. The gradual appearance of nanobacteria-like particles in incubated human serum as well as the changes seen with their size and shape can be influenced and explained by introducing varying levels of CO_2 and $NaHCO_3$ as well as other conditions known to influence the precipitation of $CaCO_3$. Western blotting reveals that the monoclonal antibodies, claimed to be specific for nanobacteria, react in fact with serum albumin. Furthermore, nanobacteria-like particles obtained from human blood are able to withstand high doses of γ-irradiation up to 30 kGy, and no bacterial DNA is found by performing broad-range PCR amplifications. Collectively, our results provide a more plausible abiotic explanation for the unusual properties of purported nanobacteria.

human serum albumin | hydroxyapatite | pathogenesis

Research on nanobacteria has gained momentum in recent years with an increasing number of reports showing their occurrence in human diseases. Nanobacteria were implicated in gallbladder (1) and renal stone formations (2), polycystic kidney diseases (3), rheumatoid arthritis (4), coinfections with HIV (5), ovarian (6) and nasopharyngeal cancer (7), Alzheimer's disease (8), and chronic prostatitis (9). Miller *et al.* (10) from the Mayo Clinic recently cultured nanobacteria from calcified arteries and showed that these entities costained for DNA and nanobacteria antigens. In view of their capacity to nucleate hydroxyapatite (HAP) (2), nanobacteria have been heralded as a potential etiological factor of extraskeletal calcification (11).

The intriguing characteristics of human nanobacteria include extremely small size from 80 to 500 nm (12), 0.2-μm filterability (3), widespread abundance in animals and humans (11), as well as nucleation of HAP (2). These unusual characteristics actually lead to the suggestions that nanobacteria may represent an overlooked primitive form of life (13) with the smallest cellular dimension known on Earth (14). Similar structures described as "nannobacteria" were also reported to abound in calcium carbonate (15) and sulfides sediments (16) where they were seen as overlooked factors affecting geochemical cycles. Other authors reported the presence of so-called "nanobes," a purported form of nanoscopic actinomycete-like microorganisms, which supposedly grow on Triassic and Jurassic sandstones (17). Similar nanoparticles and polycyclic aromatic hydrocarbons were also detected in meteorite fragments from Mars, leading to the hypothesis that these structures represent fossilized bacteria (18). This finding prompted the National Academy of Sciences (NAS) to call for a workshop seeking to define the minimal bacterial size compatible with life (19) and the National Aeronautics Space Association (NASA) to determine the relevance of nanobacteria in exobiology and astronaut infections (20). As a result, researchers at NASA have found that human nanobacteria multiply faster in a low-gravity environment, an observation deemed to be linked to the high risk of developing kidney stones for astronauts (20). Clinical treatments commercialized by Nanobac Life Sciences, a company owned in part by the discoverers of nanobacteria, are already being promoted on the basis of the eradication of these potentially living and pathogenic microorganisms (9, 21).

The hypothesis that nanobacteria might represent living microorganisms is based on an unusual set of microbiological characteristics that include their slow growth in liquid cell culture media (20), expression of specific antigens (3), and typical bacterial appearance (2). However, observations of abiotic substrates would caution against assigning any life activity to unusual biological entities because certain chemical substrates may adopt the appearance of simple microorganisms (22). In fact, Cisar *et al.* (23) produced a HAP substrate morphologically suggestive of, but far from being identical to, nanobacteria preparations. More importantly, they showed that HAP could be propagated similarly to a bacterial subculture; they also reattributed the published nanobacteria 16S rDNA sequence to an occasional contaminant of PCR reagents. However, the nanobacteria field has largely ignored these important findings and, in recent years, has continued to host a flurry of research (10, 20) and review papers (11, 24) that purport to find a pathogenic role for nanobacteria in various disease processes.

In view of the importance of the nanobacteria concept to biology and medicine and the fact that they are the basis of several ongoing human therapy trials, we reasoned that the clarification over the nature of nanobacteria must be addressed first. Based on the data reported here, we show that the biology of purported nanobacteria can actually be explained by an abiotic mechanism involving gradual precipitation of $CaCO_3$ in biological specimens.

Results and Discussion

Morphology of Purported Nanobacteria Cultured from Human Blood. We first repeated the culture of purported nanobacteria from healthy human serum. To distinguish our findings from those in the literature, we refer to our own material as nanobacteria-like particles (NLP). The criteria used to confirm that we reproduced the phenomenology of putative nanobacteria were based on earlier publications (2, 20). They included the typical bacteria-like morphology seen by electron microscopy, slow doubling-

Author contributions: J.M. and J.D.-E.Y. designed research; J.M. performed research; J.M. and J.D.-E.Y. analyzed data; and J.M. and J.D.-E.Y. wrote the paper.

The authors declare no conflict of interest.

This article is a PNAS Direct Submission.

†To whom correspondence should be addressed. E-mail: jan.martel@usherbrooke.ca.

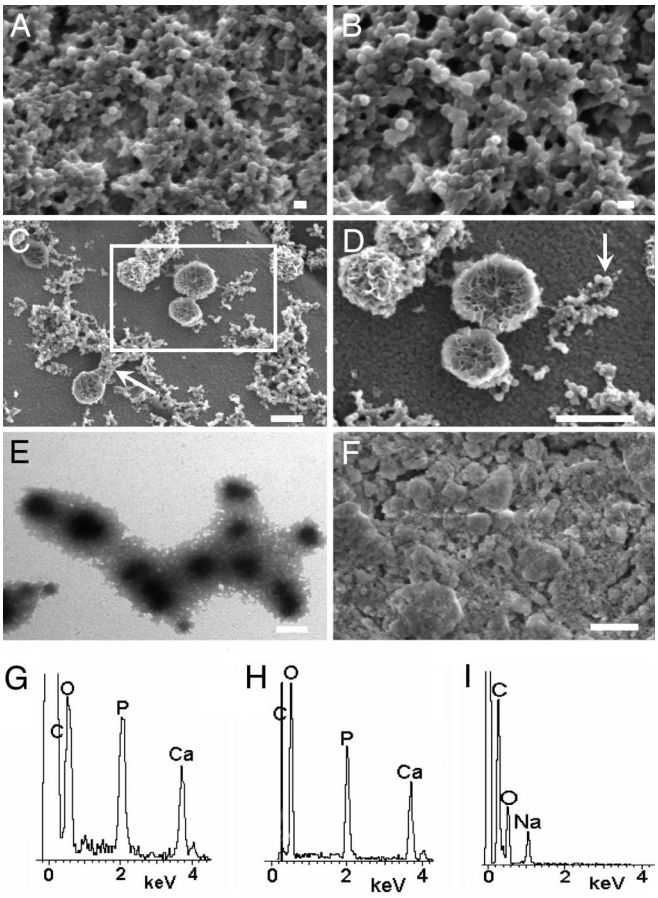

Fig. 1. Morphology and surface composition of nanobacteria-like particles. (*A*) SEM of NLP obtained by incubating healthy human serum diluted to 10% in DMEM showing colonies of coccoid bacteria-like formations. (*B*) Close-up SEM of NLP showing their diameter size between 500 and 1,000 nm. (*C*) SEM of a mixture of small NLP and larger shelter-like forms. The arrow shows the continuation between small and large forms. The square represents the section magnified in *D*. (*D*) Close-up SEM of large shelter-like formations showing their porous structure. The arrow indicates a small cell division-like formation. (*E*) Negative-stain TEM of NLP with an electron-dense core after incubation in DMEM for 1 month. (*F*) SEM of control HAP. (*G*) EDX spectrum of NLP obtained from human serum incubation. (*H*) EDX of control HAP. (*I*) EDX of NLP obtained by incubating the liquid fraction of the clotted blood (see *Materials and Methods*) reveals the absence of calcium and phosphate peaks. [Scale bars: 1 μm (*A* and *B*); 10 μm (*C*, *D*, and *F*), and 100 nm (*E*).]

time of 3 days, detection of HAP, and staining with nanobacterial antibodies.

After 5 days of serum incubation, a white precipitate formed and adhered on the bottom of each flask. When examined by scanning electron microscopy (SEM) and transmission electron microscopy (TEM), the precipitate was seen to consist of particles with a size ≈500 nm (Fig. 1 *A*, *B*, and *E*), an observation consistent with normal bacterial morphology, which peaks at one particular size specific to the strain on hand. Some forms resembled cells undergoing division (Fig. 1*D*, arrow). Larger so-called "shelter-like forms" of several micrometers were also observed among these particles, albeit in much smaller number (Fig. 1 *C* and *D*), again consistent with earlier reports (2). Although these structures were initially described as shelters for actively growing nanobacteria (2), they were seen in our own studies as being porous structures with partial crystallization inside. The smooth continuity between the larger forms and the colonies of NLP suggests that they may have the same composition (Fig. 1*C*, arrow).

Energy-dispersive x-ray (EDX) spectra analysis of NLP revealed high peaks of calcium and phosphorus (Fig. 1*G*). In fact, the EDX spectrum and atomic P:Ca ratio (1.5 ± 0.1, based on three samples) associated with these NLP preparations (Fig. 1*G*) resemble those seen with control HAP (P:Ca ratio of 1.62 ± 0.08, based on three samples; Fig. 1*H*), indicating that HAP accumulates around these entities in accordance with earlier reports (2, 20). However, the morphology of pure HAP crystals (Fig. 1*F*) was markedly different from that of NLP (Fig. 1 *A–D*); that is, no distinct bacteria-like shapes were seen in control HAP specimens. These observations indicated that the presence of HAP may not be necessary for the formation of NLP. In fact, we noticed that some types of serum fractions used (*Materials and Methods*) did not yield HAP. Indeed, the EDX spectrum of NLP cultured from the liquid fraction of the clotted blood revealed a simple profile of carbon, oxygen, and sodium at atomic C:O:Na ratios of 64:32:4 (Fig. 1*I*). No phosphorus was detected that might indicate the presence of HAP. It appears that the formation of HAP around NLP can be inhibited by blood proteins once NLP have taken their round morphology. Therefore, HAP may not be a necessary component of nanobacteria because it appears to deposit onto NLP only under particular circumstances.

Calcium Carbonate Nanoparticles Morphologically Similar to Nanobacteria-Like Particles. As shown above, it became clear that HAP could not account *per se* for the morphological features of NLP. We therefore sought to study other simple calcium compounds that might assume forms comparable with NLP. In particular, we focused on calcium compounds that are likely to precipitate in the presence of biological fluids like serum. Preliminary experiments showed that, of the compounds examined ($CaCO_3$, $CaCl_2$, and various calcium phosphate combinations), only $CaCO_3$ gave morphologies similar to nanobacteria.

To induce $CaCO_3$ precipitation and the formation of $CaCO_3$ nanoparticles that could in turn be compared with NLP preparations, we used a number of simple chemical reactions known to yield $CaCO_3$. Shown here are the results of one such reaction, involving the addition of $(NH_4)_2CO_3$ crystals to a calcium salt solution or, simply, the mixing of equal quantities of $(NH_4)_2CO_3$ and $CaCl_2$. Common $CaCO_3$ crystal polymorphs resembling vaterite, aragonite, and calcite were observed in the precipitate. We verified by EDX that the $CaCO_3$ crystals prepared did not have impurities >0.5% of the crystal weight (Fig. 2*H*). When $CaCO_3$ was prepared in DMEM, round nanostructures completely different from calcite crystals were obtained (Fig. 2 *A* and *B*). These $CaCO_3$ structures had a round morphology and appeared to have a membrane-like contour when observed under optical microscopy (Fig. 2*C*; compare with calcite crystals seen in Fig. 2*G*). They were remarkably similar to the structures described as nanobacteria observed in human and geological samples (see refs. 2 and 15; compare also Fig. 2 *A* and *B* with Fig. 1 *A* and *B*). These round structures of $CaCO_3$ are probably caused by the presence of an amorphous phase of $CaCO_3$ that surrounds the crystals, as described in ref. 25. In the absence of culture medium like DMEM, round $CaCO_3$ particles were apparent within 10 min after mixing together $(NH_4)_2CO_3$ and $CaCl_2$, and with time, these forms steadily converted into the more common $CaCO_3$ crystals mentioned earlier. However, in the presence of DMEM, these round nanostructures were preserved; they did not convert into calcite even after prolonged incubation in DMEM overnight.

Surprisingly, some of the $CaCO_3$ structures were remarkably similar to cells undergoing binary fission and budding (Fig. 2 *C–F*). Symmetrical division forms with an internal septum were frequently observed (Fig. 2*D*) as well as structures resembling divisions occurring simultaneously in vesicular forms (Fig. 2*C*, *arrow*), observations that were made earlier with nanobacteria preparations (14). Because $CaCO_3$ spontaneously precipitates in saturated solutions, the appearance of cellular divisions and

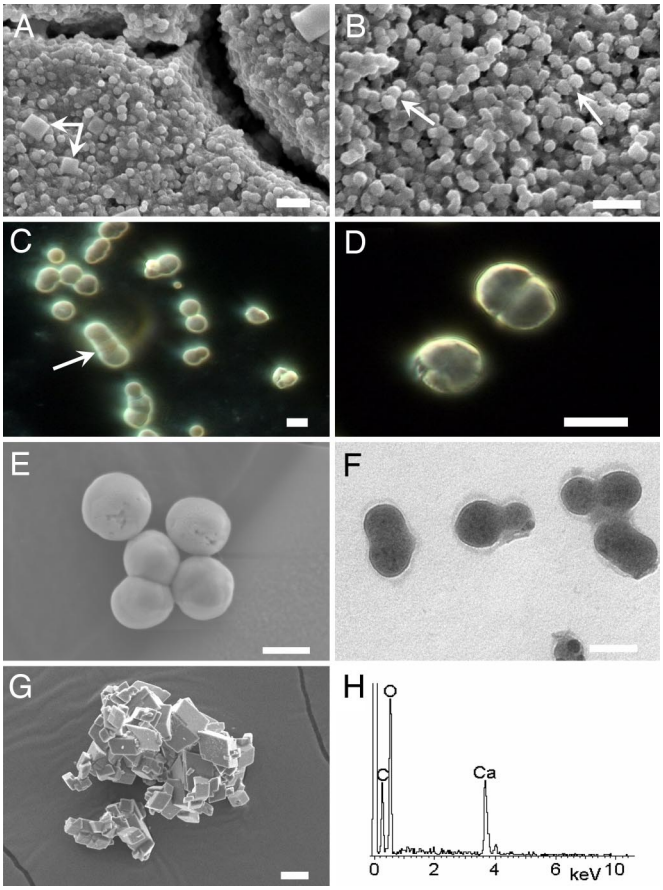

Fig. 2. Calcium carbonate nanoparticles prepared *in vitro* are similar to NLP. (*A*) SEM of $CaCO_3$ nanoparticles prepared from the diffusion of $(NH_4)_2CO_3$ crystal vapors into a solution of 1 M $CaCl_2$. Coccoidal bacteria-like structures with a narrow size range are observed along with euhedral calcite crystals (arrows). (*B*) SEM of $CaCO_3$ nanoparticles prepared by diluting 1 M $(NH_4)_2CO_3$ and 1 M $CaCl_2$ 1:100 in DMEM. Arrows indicate cell division-like forms. (*C*) Dark-field microscopy of larger $CaCO_3$ crystals prepared by mixing 1 M $(NH_4)_2CO_3$ and 1 M $CaCl_2$ 1:1 showing cellular appearance and division-like formations. The arrow shows a segmented cell division-like form. (*D*) Dark-field microscopy of a $CaCO_3$ binary fission-like form along with a vesicle-like form reminiscent of a single cell. (*E*) SEM of large $CaCO_3$ particles showing rounded-edge vesicles and a cell division-like formation. (*F*) Negative-stain TEM of $CaCO_3$ nanoparticles prepared in DMEM. (*G*) SEM of control $CaCO_3$. (*H*) EDX of $CaCO_3$ nanoparticles prepared by mixing 1 M $(NH_4)_2CO_3$ and 1 M $CaCl_2$ 1:1. [Scale bars: 1 μm (*A* and *B*), 5 μm (*C–E*), 100 nm (*F*), and 10 μm (*G*).]

budding can be understood as the juxtaposition of aggregating amorphous forms. Although cellular division formations had been used to support the notion that nanobacteria are living cells able to divide (14), these forms can be actually seen here with $CaCO_3$ nanoparticles prepared *in vitro*.

These results suggested that the growth medium may contain factor(s) that slow down or inhibit the kinetics of formation of $CaCO_3$ crystals, favoring instead the formation of round amorphous structures that had earlier been misconstrued to represent nanobacteria. These same results also prompted us to use DMEM and serum in various proportions in an attempt to mimic and reproduce the whole morphological array of shapes that have been used in the past to support the notion that nanobacteria are growing entities (2). Accordingly, by using DMEM to dilute and mix solutions of $(NH_4)_2CO_3$ and $CaCl_2$, we were indeed able to produce stable amorphous $CaCO_3$ nanoparticles in the size range of NLP (50–800 nm) (Fig. 2*B*). Similar results were obtained with serum and other culture media as well as with a wide range of dilutions (see *Materials and Methods*; data not shown). These results suggested that complex biological solutions or fluids may contain components that generate amorphous $CaCO_3$ aggregates that bear striking resemblance to the purported nanobacteria presented in the literature (2, 3).

To explore this possibility further, we tested whether either proteins or other divalent cations like Mg^{2+} might be responsible for the inhibition of $CaCO_3$ crystal formation. We tested solutions of purified albumin or Mg^{2+} compounds in the presence of $(NH_4)_2CO_3$ and $CaCl_2$ (see *Materials and Methods*). In both cases, we were able to obtain stable amorphous $CaCO_3$ nanostructures as seen in Fig. 2*A* that are similar to NLP obtained in the presence of serum (Fig. 1 *A* and *B*). It is unclear at this time how either albumin or Mg^{2+} inhibits the $CaCO_3$ crystal formation, giving in turn rise to the amorphous NLP. When no $CaCO_3$ crystal inhibitors (e.g., proteins and Mg^{2+}) were present in the $CaCO_3$ solutions tested here, round structures were seen to grow to diameters of several micrometers (Fig. 2 *C–E*) and eventually to convert to calcite crystals (data not shown). Thus, the rare larger shelter-like forms described in NLP preparations (Fig. 1 *C* and *D* and ref. 2) and seen in our $CaCO_3$ preparations (Fig. 2 *C* and *D*) are probably the result of a similar process.

Influence of Atmosphere Composition and Sodium Bicarbonate Concentration on Nanoparticle Formation. We next explored the physiological relevance of these findings in the context of human biology. We focused on the following common biological reactions, known to produce $CaCO_3$ in blood as well as in all biological tissues:

$$CO_2 + H_2O \leftrightarrow H_2CO_3 \quad [1]$$

$$H_2CO_3 + H_2O \leftrightarrow H_3O^+ + HCO_3^- \quad [2]$$

$$HCO_3^- + H_2O \leftrightarrow H_3O^+ + CO_3^{2-} \quad [3]$$

$$Ca^{2+} + CO_3^{2-} \leftrightarrow CaCO_3 \quad [4]$$

In the case of human serum culture, for example, $CaCO_3$ can precipitate by the reaction of Ca^{2+} and CO_3^{2-} (Reaction **4**) derived from the dissociation of H_2CO_3 in water as shown in Reactions **2** and **3**.

The growth of NLP in culture had been monitored through an increase in optical density at 650 nm during incubation (20). We used the same method coupled to SEM observations (as described in ref. 26) to study the impact of various treatments on their growth. We first confirmed that DMEM alone did not produce any increase of optical density after prolonged incubation up to 1 month, in line with published results (20), indicating that there is the need for some seeding factor in the medium to generate the published optical density change. This change in optical density could be induced by seeding DMEM with a 10% human serum inoculum (Fig. 3*A*). When the DMEM/serum mixture was incubated with 5% CO_2 (see *Materials and Methods*), we obtained the characteristic slow increase in optical density, which in the past had been used to support the notion that nanobacteria reproduce slowly, with a doubling time of 3 days (Fig. 3*A*; see also ref. 20). By replacing this same cell culture atmosphere of 5% CO_2 with 100% inert gas, such as argon, the increase in optical density was markedly increased (Fig. 3*A*), concordant with the expected shift in the equilibrium of Reactions **1–4** shown above, which in this situation would favor the precipitation of $CaCO_3$. In contrast, by incubating blood samples in 100% CO_2, the formation of $CaCO_3$ nanoparticles was markedly inhibited compared with standard cell culture conditions (Fig. 3*A*). SEM observations done on comparable NLP samples confirmed that these optical density measurements were representative of the number of nanoparticles (data not shown).

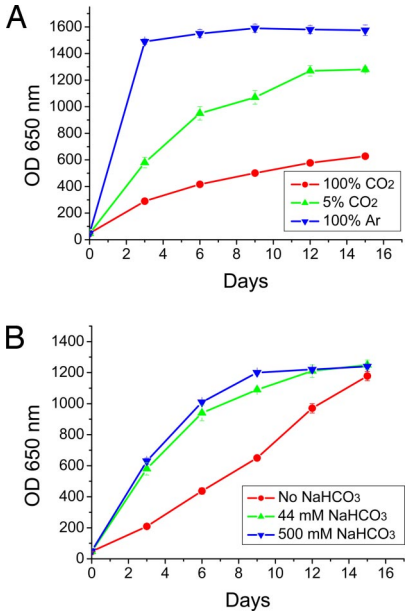

Fig. 3. Influence of carbon dioxide and sodium bicarbonate on the culture of NLP. (*A*) Standard cell culture incubation of healthy human serum diluted 10% in DMEM, incubated with 5% CO_2, 100% CO_2, or 100% argon. Sample preparations and optical density reading at 650 nm (OD 650 nm) are as described in *Materials and Methods*. (*B*) Influence of different levels of $NaHCO_3$ (*Inset*) on the number of NLP found in human serum cultures.

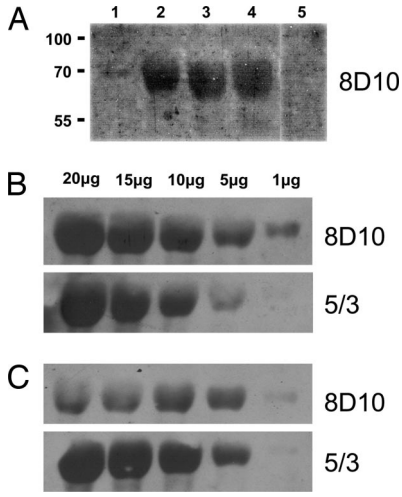

Fig. 4. Reaction of nanobacterial monoclonal antibodies 8D10 and 5/3 with NLP cultures and pure albumin fractions. (*A*) Western blotting done with 8D10 on pelleted, 1-month-old NLP (lane 1), supernatant of 1-month-old NLP culture (lane 2), healthy whole human blood incubated for 1 month (lane 3), and fresh, healthy whole human blood (lane 4). Note a prominent band of 68 kDa for all four fractions as opposed to the protein extract from 293T cells used as control (lane 5). Only fraction from lane 1 but not fractions from lanes 2–5 contained NLP when observed by SEM. (*B*) Western blotting performed with antibodies 8D10 and 5/3 on different amounts of pure HSA that shows the same unique band of 68 kDa. (*C*) Immunoblotting done on different amounts of BSA that give the corresponding 68-kDa band.

No difference was noted in EDX surface composition spectra on precipitates collected from the various treatments (data not shown), indicating that the NLP seen in the various experiments were chemically similar.

The formation of $CaCO_3$ nanoparticles in DMEM, after serum inoculation, was also influenced by adding or removing $NaHCO_3$ buffer in the culture medium (Fig. 3*B*). The DMEM used in our experiments contained 44 mM $NaHCO_3$; we compared the changes in optical density seen with this concentration of $NaHCO_3$ against incubation in culture medium containing either 500 mM or no $NaHCO_3$. In all experiments, 5% CO_2 was used. As shown in Fig. 3*B*, a decrease in the number of nanoparticles was observed when $NaHCO_3$ was removed from the culture medium. However, 500 mM $NaHCO_3$ produced a slight increase in optical density (Fig. 3*B*); this initial increase in optical density leveled off after day 12, and by day 16, all three conditions produced comparable optical densities (Fig. 3*B*), indicating that HCO_3^- might have reached comparable concentration levels in all three experimental conditions through the gradual equilibration of CO_2 in the medium.

The pH of the culture was shown to increase up to a maximum of 1.5 pH units with the argon and 500 mM $NaHCO_3$ treatments and, likewise, to decrease by a maximum of 1.5 pH units with the CO_2 and no $NaHCO_3$ treatments (experiments depicted in Fig. 3 *A* and *B*). This pH variation is consistent with the maintenance of equilibrium seen with Reactions **1**-**4** shown above to explain the formation of calcium carbonate in our system. For instance, an increase in carbon dioxide leads to the accumulation of carbonic acid in Reaction **1**, which in turn increases the amount of H_3O^+ in Reactions **2** and **3**, thereby decreasing the pH and favoring the dissolution of $CaCO_3$ (Reaction **4**). An increase in inert gas such as argon reverses this process by decreasing the concentration of CO_2 (Reaction **1**).

Together, these experiments point to a chemical model for the formation of the NLP. We were able to control the formation of precipitating NLP in culture based on our hypothesis that the core of these entities represents $CaCO_3$. It is apparent that such a marked increase in growth in an atmosphere of inert gas or after the addition of $NaHCO_3$ cannot be attributed to the stimulation of a living microorganism.

Nanobacteria-Specific Antibodies React with Human Serum Albumin (HSA). We were also intrigued by earlier publications describing the use of monoclonal antibodies specific for nanobacteria, now commercially available through Nanobac Oy (3, 10). These antibodies were obtained from splenocyte hybridoma cells of mice that were immunized with purified nanobacteria of bovine origin and fused with the myeloma strain P3 × 63-Ag-8.653 (10). They are thought to react with a bacterial porin-like protein synthesized by these nanoentities (3). Surprisingly, experiments attempting to identify the exact nature of this antigenic reactivity have never been reported, and yet the same antibodies were used in past studies to affirm the presence of nanobacteria (3, 5, 7). We first observed that antibody 8D10 reacted with NLP obtained after pelleting the material from 1-month-old culture (Fig. 4*A*, lane 1). This same pellet revealed an abundance of NLP when observed under SEM (data not shown). The molecular mass of the single band detected was 68 kDa (lane 1). It should be noted that most studies using 8D10 and 5/3 antibodies have actually focused on ELISA (5) and tissue or cell culture immunostaining (7). Miller *et al.* (10) showed that the antibody 8D10 reacts against one single band of 50 kDa from cell pellets prepared under reducing and denaturing conditions comparable with our experiments.

To address further the issue of specificity, we reacted antibody 8D10 against the supernatant of the same 1-month-old NLP used for Fig. 4*A*, lane 1. Because this supernatant, when concentrated and observed by SEM, did not reveal NLP, we expected to find little or no reactivity on the immunoblot. To our surprise, we observed the same reactive band of 68 kDa (Fig. 4*A*, lane 2). These results suggested to us that 8D10 might react to other control specimens as well. In fact, a control sample of whole blood, aged for 1 month without any further inoculation into medium, treatment, or extraction, and yielding no SEM detec-

tion of NLP, revealed the same band when reacted on the immunoblot with 8D10 (Fig. 4*A*, lane 3). Moreover, even fresh blood samples reacted in the same way (Fig. 4*A*, lane 4); here, too, there was no detection of NLP when observed under SEM (data not shown). We noticed that only protein samples derived from serum-free cell extracts did not react with 8D10 (exemplified by Fig. 4*A*, lane 5).

These results prompted us to speculate whether the reactive proteins might not in fact represent common human proteins that associate with $CaCO_3$ nanoparticles. Our earlier results suggested that, given its molecular mass, serum albumin, the most abundant protein in the plasma, might serve as a good candidate. 8D10 and 5/3 monoclonal antibodies were shown in fact to react with both pure HSA and BSA in a stoichiometric fashion (Fig. 4 *B* and *C*). It appears that the high degree of similarity between HSA and BSA (27) makes it possible for the antibodies to react with both proteins. It is possible that these monoclonal antibodies may react with minor bands not detected in our immunoblot experiments. However, the prominence of the albumin reactivity makes it unlikely that it would not interfere with the antibody staining under any foreseeable circumstances.

The presence of albumin and possibly of other binding proteins in the NLP seems to make sense because they may serve as modulators or inhibitors of $CaCO_3$ crystallization, which in turn may be responsible for generating NLP. It is not clear how tightly albumin binds to the nanoparticle complex and what role it may have in the assembly of the nanoparticle, but already some hints can be obtained through preliminary experiments. NLP that had been pelleted, washed, and incubated with 3 M EDTA overnight retained their amorphous nanobacteria-like morphology as well as a dominant albumin band that reacted strongly to the two monoclonal antibodies (data not shown). These observations suggest that the presence of proteins early in the $CaCO_3$ nucleation process may result in the formation of an insoluble matrix that resists decalcifying treatments. On the basis of these results, we must conclude that these antibodies do not specifically recognize antigens produced by nanobacteria as reported earlier (3). They were instead found to react with serum albumin, and although this protein may be associated with NLP, it certainly cannot be used as a specific biomarker for a living microorganism.

Characteristics of NLP Irreconcilable with Those of Living Organisms. We observed NLP in the culture of every healthy human serum tested ($n = 20$), an observation in line with another study that reported that 90–100% of animal sera from cattle, goats, cats, and dogs gave similar nanoparticles (28). Thus, NLP formation would appear to be unrelated to pathogenesis. Besides, γ-irradiation of human serum samples up to 30 kGy before culture did not prevent the growth of NLP in our hands, contrary to earlier reports (2). Furthermore, we found no bacterial 16S rDNA from PCR amplifications conducted on NLP preparations, despite numerous attempts (data not shown). Other groups also failed to show the presence of nucleic acids within putative nanobacteria using PCR (28, 29) as well as spectroscopy and staining methods (23). These results rule out the possibility that these entities rely on the duplication of DNA or RNA for their propagation.

We also obtained NLP from serum diluted in DMEM and filtered through 0.1-μm pore size membranes (see *Materials and Methods*; data not shown). This result implies that the replicative unit or nucleating agent responsible for such a growth is smaller than 100 nm in diameter. Because an earlier workshop commissioned by the NAS had suggested that the minimal cellular size of life on Earth must exceed 200 nm in diameter to harbor the cellular machinery based on DNA replication (19), it is unlikely that nanobacteria represent living entities unless they contain some other type of replicating mechanism. The amorphous $CaCO_3$ nucleation hypothesis described in this article provides an alternative abiotic view that can now be used to reconcile the phenomenology of NLP with accepted definitions of life.

In summary, we reproduced the earlier nanobacteria-related observations by incubating human serum in cell culture conditions. However, we observed that HAP cannot by itself explain the dynamic process responsible for the formation of these nanoentities. By searching for simple chemicals likely to precipitate from biological fluids, we found that $CaCO_3$ can adopt morphologies remarkably similar to NLP. In fact, these amorphous $CaCO_3$ complexes can easily form cellular division-like structures reminiscent of living microorganisms. We were also able to influence the speed with which NLP could be formed by varying the substrates needed for $CaCO_3$ precipitation in culture. Besides, the lack of specificity of nanobacteria antibodies casts doubts on the validity of previous results and warrants against their use as a diagnostic, and perhaps therapeutic, tool in medicine. Our results also point toward the possibility that formations such as those reported in meteorites (18) and geological samples (15, 16) are the result of a similar process.

Materials and Methods

Culture of NLP. NLP were cultured from human serum as described in ref. 2. Briefly, healthy human blood samples ($n = 20$) were aseptically drawn into sterile Vacutainer tubes without anticoagulant (Becton Dickinson) by a conventional venipuncture technique. The clear serum was prepared by centrifuging the clotted blood at $1,500 \times g$ for 5 min and by diluting the supernatant 1:10 in DMEM (Invitrogen) which, when indicated, contained different amount of $NaHCO_3$. When the mixtures of serum and DMEM were incubated with different gases or various amounts of $NaHCO_3$, the pH was adjusted to 7.4 before incubation. The solution was filtered through a 0.2-μm or 0.1-μm pore size sterilizing membrane before incubation in conventional cell culture conditions (37°C; 5% CO_2, 95% air) for 1 month. The culture of NLP was also performed by using the cloudy liquid fraction of the clotted blood (without centrifugation); this fraction was diluted 1:10 in DMEM and processed as described above. This culture method was used to obtain NLP from every blood sample, to show that HAP is not a necessary component of NLP as well as for spectroscopy measurements. Spectroscopy measurements were performed as described in ref. 20. To verify the influence of inert gas and CO_2 on NLP formation, culture flasks and 96-well culture plates inoculated with human serum diluted 10% in DMEM were incubated in a hypoxic chamber (Billups-Rothenberg). Sterile argon or CO_2 was flushed inside the jar at a flow rate of 20 liters/min for two periods of 10 min separated by a 1-h interval. To verify the impact of γ-irradiation on the growth of NLP, 10% filtered human serum in DMEM was γ-irradiated up to 30 kGy (Institute of Nuclear Energy Research, Atomic Energy Council, Taiwan) before culture.

Preparation of $CaCO_3$ Nanoparticles. $CaCO_3$ nanoparticles were prepared by diffusion of $(NH_4)_2CO_3$ crystal vapors into a 1 M $CaCl_2$ solution as described in ref. 30. To prepare small uniform $CaCO_3$ nanoparticles, 1 M $CaCl_2$ was first mixed with $MgCl_2$ to obtain a Ca:Mg ratio of 1:1 to 1:10. Small $CaCO_3$ nanoparticles were also obtained by using DMEM to dilute 1 M $(NH_4)_2CO_3$ and 1 M $CaCl_2$ in ratios ranging from 1:50 to 1:500. The formation of larger amorphous $CaCO_3$ particles and common crystals of $CaCO_3$ was studied by mixing $(NH_4)_2CO_3$ 1 M with $CaCl_2$ 1 M in a 1:1 ratio. We also examined $CaCl_2$, $CaHPO_4$, $Ca_4O(PO_4)_2$, $Ca_3(PO_4)_2$, $Ca_{10}(PO_4)_6(OH)_2$, Na_2CO_3, and Na_3PO_4 by dissolving them in water or DMEM at concentrations varying from 1 to 100 mM and incubating them for 1 month. To study the influence of proteins and serum on the formation of $CaCO_3$ nanoparticles, whole serum or 10% serum in DMEM was used to dilute equal amounts of 1 M $(NH_4)_2CO_3$ with 1 M $CaCl_2$ in ratios ranging from 1:10 to 1:500. The role of proteins in the formation of $CaCO_3$ nanoparticles was studied by adding HSA at final concentrations varying from 0.1 to 1 mg/ml.

Optical Dark-Field Microscopy, TEM, and SEM. SEM and TEM sample preparation was described earlier (26). A 1230 TEM (JEOL) and S3000N SEM (Hitachi) were used. EDX spectra were acquired with an EMAX Energy EX-400 EDX device (Horiba). EDX spectra of NLP from human serum were obtained directly from pelleted, 1-month-old, culture material. For optical microscopy, homogenized $CaCO_3$ nanoparticles were observed without fixation or staining with a BX-51 optical microscope (Olympus) and dark-field condenser (CERBE). Images were acquired by using a KY-F55 color camera (JVC).

Western Blotting. NLP from human serum were prepared as for electron microscopy from 1-month-old culture. After two washing steps in water with centrifugation at 16,000 × *g* for 10 min, the following samples were solubilized in reducing Laemmli buffer: pelleted NLP, supernatant of the same 1-month NLP culture, 1-month-old whole-blood sample, and fresh human blood. BSA and HSA were purchased from Sigma; the negative control for nonspecific binding consisted of a protein extract from 293T human cells. Primary antibodies 8D10 and 5/3 (Nanobac Oy) were dissolved 1:1,000, and anti-mouse horseradish peroxidase-coupled secondary antibody (Amersham Biosciences) was diluted 1:2,000; both were diluted in blocking solution. An ECL Western blot detection kit (Amersham Biosciences) was used according to the manufacturer's recommendations.

DNA Extraction and PCR Amplifications. DNA extraction was performed from NLP pellet and supernatant by using the method of Higuchi (31). The broad-range 16S rDNA PCR amplification protocol used was described in ref. 32. Positive, negative, and spiked controls containing both the NLP sample and positive-control template were used to rule out the presence of PCR inhibitors in blood preparations.

ACKNOWLEDGMENTS. We thank Chin-Ming Hung, Daniel Sdicu, Jyo-Jen Ho, Ka-Po Tse, Hsin-Pai Li, and Prof. Yu-Sun Chang for technical help and Dr. Chia C. Pao for guidance and helpful discussions. This work was supported by Primordia Institute of New Sciences and Medicine and by Chang Gung University Grant FMRPD2T02.

1. Wang L, *et al.* (2006) An animal model of black pigment gallstones caused by nanobacteria. *Dig Dis Sci* 51:1126–1132.
2. Kajander EO, Ciftcioglu N (1998) Nanobacteria: An alternative mechanism for pathogenic intra- and extracellular calcification and stone formation. *Proc Natl Acad Sci USA* 95:8274–8279.
3. Hjelle JT, *et al.* (2000) Endotoxin and nanobacteria in polycystic kidney disease. *Kidney Int* 57:2360–2374.
4. Tsurumoto T, Matsumoto T, Yonekura A, Shindo H (2006) Nanobacteria-like particles in human arthritic synovial fluids. *J Proteome Res* 5:1276–1278.
5. Sommer AP, Milankovits M, Mester AR (2006) Nanobacteria, HIV and magic bullets: Update of perspectives 2005. *Chemotherapy* 52:95–97.
6. Hudelist G, *et al.* (2004) Presence of nanobacteria in psammoma bodies of ovarian cancer: Evidence for pathogenetic role in intratumoral biomineralization. *Histopathology* 45:633–637.
7. Zhou HD, *et al.* (2006) Intracellular colocalization of SPLUNC1 protein with nanobacteria in nasopharyngeal carcinoma epithelia HNE1 cells depended on the bactericidal permeability increasing protein domain. *Mol Immunol* 43:1864–1871.
8. Kajander EO, Liesi P, Ciftcioglu N (1993) *Virus and Virus-Like Agents in Diseases. Second Karger Symposium*, eds Zinkernagel RM, Stauffacher W (Karger, Basel), pp 41–45.
9. Shoskes DA, Thomas KD, Gomez E (2005) Anti-nanobacterial therapy in men with chronic prostatitis/chronic pelvic pain syndrome and prostatic stones: Preliminary experience. *J Urol* 173:474–477.
10. Miller VM, *et al.* (2004) Evidence of nanobacterial-like structures in calcified human arteries and cardiac valves. *Am J Physiol* 287:H1115–H1124.
11. Kajander EO (2006) Nanobacteria: Propagating calcifying nanoparticles. *Lett Appl Microbiol* 42:549–552.
12. Ciftcioglu N, Kajander EO (1998) Interaction of nanobacteria with cultured mammalian cells. *Pathophysiology* 4:259–270.
13. Sommer A, *et al.* (2003) Living nanovesicles: Chemical and physical survival strategies of primordial biosystems. *J Proteome Res* 2:441–443.
14. Kajander EO, Kuronen I, Akerman K, Pelttari A, Ciftcioglu N (1997) Nanobacteria from blood, the smallest culturable autonomously replicating agent on Earth. *Proc Soc Photo Opt Instrum Eng* 3111:420–428.
15. Folk RL (1993) SEM imaging of bacteria and nannobacteria in carbonate sediments and rocks. *J Sediment Petrol* 63:990–999.
16. Sillitoe RH, Folk RL, Sarie N (1996) Bacteria as mediators of copper sulfide enrichment during weathering. *Science* 272:1153–1155.
17. Uwins PJR, Webb RI, Taylor AP (1998) Novel nano-organisms from Australian sandstones. *Am Mineral* 83:1541–1550.
18. McKay DS, *et al.* (1996) Search for past life on Mars: Possible relic biogenic activity in Martian meteorite ALH84001. *Science* 273:924–930.
19. de Duve C, Osborn MJ (1999) Panel 1: Discussion. *Size Limits of very Small Microorganisms*: *Proceedings of a Workshop* (National Academy Press, Washington, DC).
20. Ciftcioglu N, Haddad RS, Golden DC, Morrison DR, McKay DS (2005) A potential cause for kidney stone formation during space flights: Enhanced growth of nanobacteria in microgravity. *Kidney Int* 67:483–491.
21. Maniscalco BS, Taylor KA (2004) Calcification in coronary artery disease can be reversed by EDTA–tetracycline long-term chemotherapy. *Pathophysiology* 11:95–101.
22. Garcia-Ruiz JM, *et al.* (2003) Self-assembled silica-carbonate structures and detection of ancient microfossils. *Science* 302:1194–1197.
23. Cisar JO, *et al.* (2000) An alternative interpretation of nanobacteria-induced biomineralization. *Proc Natl Acad Sci USA* 97:11511–11515.
24. Ciftcioglu N, McKay DS, Mathew G, Kajander EO (2006) Nanobacteria: Fact or fiction? Characteristics, detection, and medical importance of novel self-replicating, calcifying nanoparticles. *J Investig Med* 54:385–394.
25. Aizenberg J, Weiner S, Addadi L (2003) Coexistence of amorphous and crystalline calcium carbonate in skeletal tissues. *Connect Tis Res* 44:20–25.
26. Vali H, *et al.* (2001) Nanoforms: A new type of protein-associated mineralization. *Geochim Cosmochim Acta* 65:63–74.
27. Carter C, Ho JX (1994) Structure of serum albumin. *Adv Prot Chem* 45:153–203.
28. Barr SC, *et al.* (2003) Detection of biofilm formation and nanobacteria under long-term cell culture conditions in serum samples of cattle, goats, cats, and dogs. *Am J Vet Res* 64:176–182.
29. Drancourt M, *et al.* (2003) Attempted isolation of *Nanobacterium* sp. microorganisms from upper urinary tract stones. *J Clin Microbiol* 41:368–372.
30. Addadi L, Moradian J, Shay E, Maroudas NG, Weiner S (1987) A chemical model for the cooperation of sulfates and carboxylates in calcite crystal nucleation: Relevance to biomineralization. *Proc Natl Acad Sci USA* 84:2732–2736.
31. Higuchi R (1989) Simple and rapid preparation of samples for PCR. *PCR Technology*, ed Erlich HA (Stockton, New York), pp 31–38.
32. McLaughlin RW, *et al.* (2002) Are there naturally occurring pleomorphic bacteria in the blood of healthy humans? *J Clin Microbiol* 40:4771–4775.